

# **Publishable Summary for EMAS project**

**Grant Agreement number: 255811EMAS**

**Project acronym: EMAS**

**Project title: Electric Motor And Sensor design and manufacture**

**Name of the scientific representative of the project's co-ordinator<sup>1</sup>, Title and Organisation:**

**Xenofon Gryllakis**

**Tel: +302105381127**

**Fax: +302105450962**

**E-mail: [gat@ieee.org](mailto:gat@ieee.org)**

---

- Executive summary

During the EMAS project, the main candidate electrical actuation technologies for high speed severe environment aerospace applications were developed, implemented and validated. The emerging motor and speed sensor designs, as well as the resulting system packaging concepts were thoroughly tested based on their electromagnetic, thermal and mechanical performance as well as their integration and expansion capabilities.

EMAS technological platform offered a panel of induction motor and permanent magnet motor designs, both integrating emerging technologies, such as magnetic material with higher magnetic properties, optimized permanent magnet machine topology for low circuit current, high performance magnetic speed sensor and system packaging concept. These features are in accordance to the modular concept of the next generation, “more-electric” aircraft and contribute significantly to the integration of compact electronic modules able to sustain high temperature severe environment, and compact and reliable permanent magnet – high speed motors, with low short circuit current design.

The overall development of design and simulation software, directly related to the prototype manufacturing procedures, the implementation of specialized experimental test benches and the introduction of state of the art magnetic and insulation materials as well as speed sensor technology in the final actuators offered significant scientific and technical contribution, that updates the technological readiness level of smart electronic sensor and motor platforms destined to electric actuator preparation.

- Summary description of project context and objectives

The EMAS project developed a state of art electric motor and sensor actuation system, in order to suppress the whole hydraulic system in aircrafts. The project was implemented in 3 WPs that led to the achievement of the EMAS project’s objectives.

WP1 (Motor and sensor preliminary design) was oriented to the better understanding of the specifications and the complex validation plan to ensure the best implementation of the new motor - sensor actuation system. Several technologies were evaluated at a high temperature and high mechanical stress level. Three phase induction motor and fractional slot concentrated winding permanent magnet motor topologies were identified as the main candidate technologies. Before their integration in the final prototype they were improved based on software aided optimization and material testing. As a result of this first WP emerged the full specification for the two next WPs.

WP 2 (Motor and sensor critical design) hosted the core development of the EMAS project and led to the creation of the new electromagnetic-electronic part of the actuator. Consequently to the importance of all the research done in high temperature – state of art – magnetic materials, low short circuit current architectures and optoelectronic - magnetic

positioning sensors, this activity was structured in 2 different tasks involving critical design of electric motor and sensor respectively:

- Task 2.1 was dedicated to the development of a new motor for this type of actuator.

As the technological platform asks for high power density-high efficiency actuator designs under heavy thermal environment, thermal robustness and efficiency of the motor was secured by introducing state of the art materials. The final selection of the proposed stator and rotor lamination was a trade of between efficiency, mechanical behaviour and commercial availability. Additional thermal stresses have been taken into consideration. Iron laminations M235-35A/35JN230 achieves the best compromise as its design delivers good efficiency levels (including switching frequency losses components) and allows for a stable enough stator tooth manufacturing. In addition the final selection of the proposed permanent magnet is a trade of between efficiency, thermal stability and mechanical behaviour. Regarding permanent material selection, NdFeB alloys have reached a maximum working temperature of 240°C and their thermal performance seems to grow more rapidly than that of SmCo. A bibliographical research has been conducted regarding the insulating materials of the actuator. The materials that were examined to withstand up to 200 °C are mainly mica based components. The final selection of the proposed insulation material is a trade-off between thermal behavior, commercial availability and space restrictions in the machine slots. For construction of the windings, specially enamelled with aromatic Polyimide round copper wires have been selected. Moreover, mica reinforced Nomex slot insulation and end winding insulation has been selected. Due to no change of lubrication requirement SKF BHTS 2RSVT bearings operating up to 6800 rpm and 200 °C have been selected. The machine cover plates have been constructed from stainless steel alloy constituting a good solution for mechanical strength requirements.

The main candidate motor topologies were also developed and validated for the specific application. A comparative analysis between permanent magnet motor and induction motor aerospace actuators has been carried out. Different combinations of rotor-stator slots for the induction motor and different winding layouts for the permanent magnet motor have been modelled and performances have been compared. The optimum induction motor configuration, featured by the absence of rotor magnetic field, required larger dimensioning and weight than the respective permanent magnet motor one, for the same thermal evacuation ratio. However, the induction motor case presented lower braking torque and short-circuit currents with respect to the permanent magnet case, leading the final choice of the actuator technology to an overall system considerations dependent problem. In the undertaken analysis the permanent magnet motor configuration was favourable by using the same thermal evacuation criterion.

Particularly, for the induction motor, conventional design principles have been followed, mainly focusing on the efficiency and the output torque. Different topologies and winding configurations suitable for the specific application have been investigated and compared, in order to identify the one exhibiting the best performance with respect to the considered specifications. The non-overlapping winding investigation has shown that

under such circumstances and topology, a non-overlapping winding is not favourable and effective for the induction motor, thus the classical winding layout has been followed. In order the induction motor to meet the requirements the whole available space, maximum length and diameter, is required to be covered taking into consideration the best performance. For the cross section of the rotor bars the NEMA design class A has been followed as the most appropriate offering higher torque capacity at lower frequency slip levels. Finally, a sensitivity analysis of the main motor parameters of the selected configuration has been performed in order to define the detailed motor design. On the contrast, for the permanent magnet motor, an analysis of the alternative machine topologies and the available winding configurations suitable for this specific application has been fulfilled focusing on the key points of performance, efficiency and reliability. The effective length of the permanent magnet machine has been configured at 40 mm, which is one third of the total available length.

Furthermore, both overlapping and non overlapping winding configurations have been investigated. The non overlapping single layer winding was considered a more favourable choice due to its underlying advantages such as lower copper losses and torque ripple. Visions of future more electric aircraft technology contain high penetrations of Fractional Slot Concentrated Winding (FSCW) Permanent Magnet Synchronous Machine (PMSM) actuators. FSCW actuators are intended to gradually replace hydraulic flight controls, allowing for both safer and "more-green" operations. This is mainly due to the advantages of low cogging torque, short end turns, high slot fill factor, as well as fault tolerance and flux-weakening favouring FSCWs to Full Pitch Concentrated Windings (FPCWs) in the respective applications.

However, fractional pitch configuration affects the performance of the actuator similarly to the case of a reduced number of turns in the winding, leading to back-EMF voltage amplitude and power-factor reduction in regard to the case of FPCWs. Such a performance related effect can be critical in aerospace applications that require actuation systems to comply with maximum efficiency and high power density specifications. As FSCW technical characteristics call for less copper, while FPCW physical characteristics call for maximum EMF per inductor, the optimum actuator topology can be a function of the application specifications. The latter has to be determined analytically. The actuator design is based on a particular optimization algorithm, developed in order to facilitate the comparative approach on the stator geometry optimization of surface PMSMs involving FPCW and FSCW configurations. More specifically, a Rosenbrock based optimization algorithm is introduced in order to minimize an application-specific penalty function through the Sequential Unconstrained Minimization Technique. The proposed formula of the penalty function includes efficiency-performance related terms, as well as technical terms, related to the manufacturing cost of each stator configuration. Proper sigma terms ensuring no violation of the optimization constraints have been also introduced. The algorithm offered stable convergence characteristics in all design cases considered.

- Task 2.2 involves the development of a new speed sensor module for the actuator.

Sensor response was characterized at high speed – high temperature operating environment and detailed design parameter values were computed for optimal steady

state - dynamic operation of the electronic speed sensor module under nominal operating conditions. Equally, improvement of the electronic part of the actuation system was done in conjunction with electromagnetic system critical design procedure. Special attention was also given to the interactive design of motor and sensor electronic parts, and all the interactions were fully taken under consideration.

Magnetic resolver technology was finally selected. After completing an investigation among the available resolvers, the Rotasyn resolver has been chosen carefully meeting all the required specifications of the EMAS technological platform. Unlike the traditional brushless resolver, the Rotasyn has both primary and secondary windings in the stator and thus no rotary transformer is required (Robinson D., Intelligent Motion System conference, Sept. 1995). The transferred energy remains magnetic from the primary coil through the air gap to the sinusoidally shaped poles of the solid rotor. The Rotasyn is similar to a rotary variable differential transformer (RVDT) in which the rotor acts as a magnetic valve completing the flux path. The total flux through the gap is constant - the rotor determines the angular position within the stator bore where the coupling occurs, and thus the relative amplitudes of the output signals. The primary coil is wound circumferentially between the two stators. The two secondary windings are wound in the stator slots in space quadrature (shifted by 90 physical degrees) similar to a traditional resolver. Hence the induced voltage amplitudes correspond to the sine and cosine of the rotor angle as in a traditional resolver.

WP3 (Motor and sensor testing and manufacturing) validated the ability of the new actuator system to perform the technological readiness level expected and enabled prototypes manufacturing. Using the validation plan determined in the WP1 through detailed bibliographical and technological survey, all specific test benches were developed. Specifically, complete power electronics and measuring suit was designed and implemented in the laboratory. Motor braking mechanism was implemented by employing high speed, digitally controllable hysteresis brakes. WP3 run simultaneously with the second half of critical design stage (WP2) and contingency planning was applied whenever the intermediate prototypes failed to meet the specifications set.

- Description of the main S&T results/foregrounds.

A comparative design of actuators for on board autonomous system applications based on induction motor and permanent magnet motor technologies is undertaken, by means of a combined electromagnetic and thermal evaluation. Initially, 3D time-stepping finite element analysis is employed for the determination of the actuators basic dimensional and operating characteristics. As the actuator thermal constraints constitute a key-feature of the respective systems, the proposed configurations are compared on the basis of equal thermal evacuation. The two configurations considered are in a next step optimized through the application of specific minimization of their performance-technical related costs. Both resulting induction motor and permanent magnet motor optimal configurations present complementary advantages for the specific class of applications. Permanent magnet machines, feature significant advantages over the other machine types. They have attracted a growing interest within the research community for actuator applications; thus enabling the thorough investigation of their operational characteristics.

However, in high performance actuation systems, where strict specifications as well as safety and reliability issues govern, further analysis of their operation is necessary. The absence of an electromagnetic excitation system improves their dynamic performance. The higher torque density and the simplification and maintenance are some of their most crucial advantages leading permanent magnet machines to be considered as an attractive option. On the contrary, the high short circuit currents due to the permanent existence of the rotor field and the high braking torque indicate some of their disadvantages combined with the significant magnet retention issue.

Another competitor in such applications is the cage induction machines; brushless machines without the presence of commutator or slip rings mainly characterized by the capability of high performance dynamic control. Owing to the dynamic progress made in the field of power electronics and control technology their application to electrical drives has increased considerably. However, induction motors present also numerous drawbacks, either constructional or operational, such as their small air gap, the lower efficiency and power factor than the synchronous motors. In order to overcome the presented disadvantages, improvements in the realm of the design process and drives have made easier and cost effective the motor operation over a large range of speeds still maintaining high efficiency and reliability.

Within EMAS project, two different machine topologies, a permanent magnet and an induction motor satisfying the specifications of specific applications, are designed and examined in a comparative approach. Finite elements are enlisted enabling to specify actuator basic features and determine the detailed machine configuration, shown in Fig. 1, applying innovative stator geometry optimization methods. The operational characteristics of the two machine topologies are analyzed for two different modes of operation, by employing finite element time-stepping technique. Moreover, due to the heavy environmental conditions in high performance applications, the contribution to the ambient temperature rise is of high importance; hence thermal analysis has also been conducted attaining for each configuration the equal thermal evacuation criterion. The two actuators are intended to be manufactured and incorporated in an actuation application.

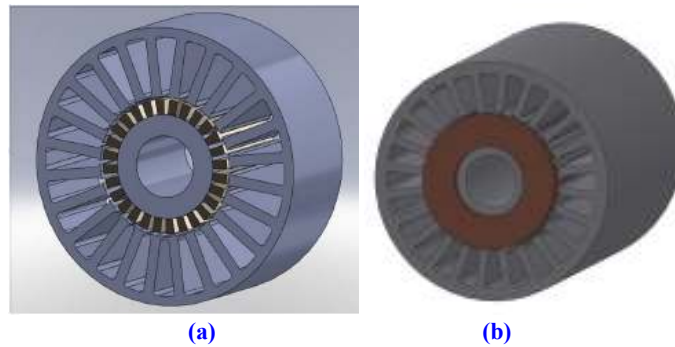


**Figure 1. 3D actuator representation models. (a) 24 slots - 28 pole PM machine. (b) 8 pole induction machine.**

- **Actuator specification**

The actuator topology has to comply with particular geometrical and electromechanical specifications. The main actuator specifications and dimensions are summarized in Table 1, for the two different modes of operation. Under normal operation the output torque is

about five times less compared to the extreme mode of operation presenting also irrespectively increase in rotor speed. Such an extreme difference in machine specifications is common in high performance applications; mainly for safety reasons due to undesirable disturbances during certain manoeuvres. Restrictions are now set by the control system capacity, dc voltage level and switching frequency.

Quantity	Value
<i>Torque, Nm</i>	<i>1.2</i>
<i>Speed, rpm</i>	<i>180</i>
<i>Maximum torque at max. speed, Nm</i>	<i>6.0</i>
<i>Maximum speed, rpm</i>	<i>6000</i>
<i>DC link voltage, V</i>	<i>270</i>
<i>Maximum outer diameter, mm</i>	<i>90</i>
<i>Maximum length, mm</i>	<i>120</i>

**Table 1. Main actuator specifications and dimensions.**

In order to determine the main motor dimensions, preliminary analysis has been carried out for the two machine types considering initially the fundamental design principles. However, each machine type demanded special attention during the design procedure satisfying the listed requirements and concerning both geometrical and spatial limitations.

- Modeling and design considerations
  - Magnetic field modelling

The time-dependent magnetic field is governed by the well known Maxwell's equation in the form of the magnetic vector potential:

$$\nabla \times \nu \nabla \times \mathbf{A} = \underbrace{\mathbf{J}_S}_{\substack{\text{conductor} \\ \text{area}}} - \underbrace{\sigma \frac{d\mathbf{A}}{dt}}_{\substack{\text{iron/air gap} \\ \text{area}}} - \underbrace{\sigma \nabla V}_{\substack{\text{electric} \\ \text{potential}}} + \underbrace{\nabla \times \mathbf{H}_C}_{\substack{\text{permanent} \\ \text{magnet}}} \quad (1)$$

where  $\nu$  is the reluctivity,  $\mathbf{A}$  is the magnetic vector potential,  $\mathbf{J}_S$  is the source current density,  $V$  is the electric potential and  $\mathbf{H}_C$  is the coercive force of the permanent magnet. The equation describing the interaction of the magnetic field with the applied machine terminal voltage is of the following form:

$$v_s = R \cdot i_s + L \cdot \frac{di_s}{dt} + \frac{l}{S} \cdot \underbrace{\left( \iint_{\Omega^+} \frac{\partial \mathbf{A}}{\partial t} d\Omega - \iint_{\Omega^-} \frac{\partial \mathbf{A}}{\partial t} d\Omega \right)}_{\text{back Electromotive Force}} \quad (2)$$

where  $R$  and  $L$  are the phase resistance and end windings inductance respectively,  $i_s$  is the stator current,  $v_s$  is the supply voltage,  $l$  is the machine length and  $\Omega^+$  or  $\Omega^-$  represent the total cross-sectional areas depending on the sign of the phase conductors current.

- Preliminary design

Particularly, for the IM, conventional design principles have been followed, mainly focusing on the efficiency and the output torque. Different topologies and winding configurations suitable for the specific application have been investigated and compared, in order to identify the one exhibiting the best performance with respect to the considered specifications. The non-overlapping winding investigation has shown that under such circumstances and topology, a non-overlapping winding is not favorable and effective for the IM, thus the classical winding layout has been followed. In order the IM to meet the requirements the whole available space, maximum length and diameter, is required to be covered taking into consideration the best performance. For the cross section of the rotor bars the NEMA design class A has been followed as the most appropriate offering higher torque capacity at lower frequency slip levels. Finally, a sensitivity analysis of the main motor parameters of the selected configuration has been performed in order to define the detailed motor design shown in Fig. 1.

On the contrast, for the PMM, an analysis of the alternative machine topologies and the available winding configurations suitable for this specific application has been fulfilled focusing on the key points of performance, efficiency and reliability. The effective length of the PM machine has been configured at 40 mm, which is one third of the total available length. Furthermore, both overlapping and non overlapping winding configurations have been investigated. The non overlapping single layer winding was considered a more favorable choice due to its underlying advantages such as lower copper losses and torque ripple.

- Geometry optimization

After completing the preliminary design process, based on analytical methods, and the winding layout selection, a particular optimization algorithm, facilitating the comparative approach on the stator geometry optimization of surface PM machines involving full pitch and fractional slot concentrated winding configurations has been employed. Fig. 2 shows the block diagram of the proposed optimization procedure. The procedure is based on the interaction between a 2-D FEM parametric model and the optimizer block.

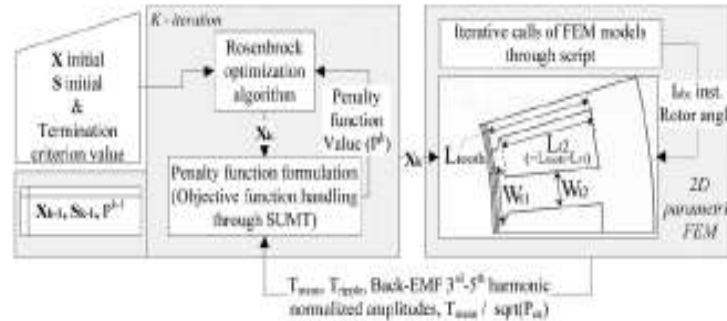


Figure 1. Block scheme of the adopted optimization algorithm.



The penalty function at the beginning of kth-iteration shown in the block scheme is given by

$$P^k(\mathbf{X}_k) = G_1 \frac{T_m(\mathbf{X}_k)}{T_m(\mathbf{X}_0)} + G_2 \frac{T_r(\mathbf{X}_k)}{T_r(\mathbf{X}_0)} + G_3 A_n(\mathbf{X}_k) + G_4 \frac{T_m(\mathbf{X}_k)}{\sqrt{P_{Cu}(\mathbf{X}_k)}} \left( \frac{T_m(\mathbf{X}_0)}{\sqrt{P_{Cu}(\mathbf{X}_0)}} \right)^{-1} + G_5 \frac{C(\mathbf{X}_k)}{C(\mathbf{X}_0)} + R^k \sum 1/(g_i(\mathbf{X}_k))$$

(3)

where  $\mathbf{X}_k$  is equal to  $[L_{tooth}^k, W_{t1}^k, W_{t2}^k]$ ,  $G_1$ - $G_5$  represent the weight coefficients,  $T_m$  and  $T_r$  represent the mean and ripple torque respectively,  $A_n$  is the 3rd and 5th normalized amplitude sum,  $g_i(\mathbf{X}_k)$  are the problem constraints and  $C$  is the total technical cost concerning the selected geometry.

- Induction motor actuator case

The most critical characteristic featuring the induction motors is the lack of excitation in the rotor side. The establishment of the rotor magnetic field demands higher current density to flow into the stator. Hence, it is reasonable that under these circumstances the IM requires larger envelope dimensions than a PM machine in order to achieve the equal output torque under the same stator current density levels. In Fig. 3 the output torque versus slip frequency is presented for different current densities and effective machine lengths considering an actual slot fill factor equal to 0.5 and constant currents.

From Fig. 3, it can be observed that the eight-pole IM design meets the specifications at the maximum available machine length of 120 mm considering that a thermally acceptable current for the normal operating conditions is of about 6 A/mm<sup>2</sup>.

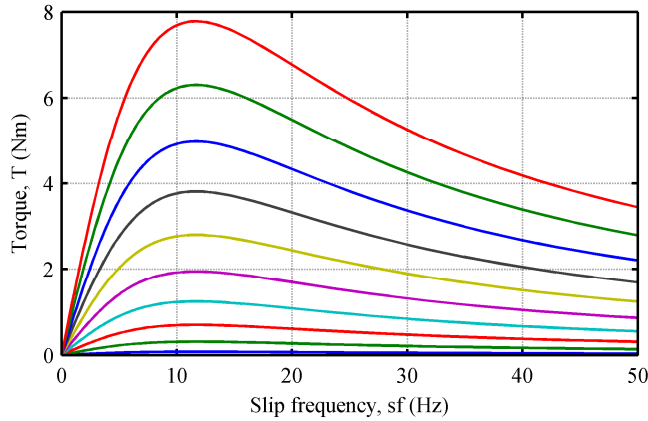


Figure 2. Instantaneous torque profile versus slip frequency for 5 to 50 Arms with 5 Arms step.

Fig. 3 shows the flux density distributions of the IM for the two modes of operation at different time sequences. The actual supplied current density is 6 A/mm<sup>2</sup> and 13 A/mm<sup>2</sup> respectively, offering the required torque levels and exploiting adequately the stator and rotor core materials thus operating at the knee of the laminations BH curve, which

constitutes a design process criterion. The normal saturation levels leads to the fact of the almost pure sinusoidal EMF. Figs. 4 and 5 illustrate the unsaturated core for the normal operation, where the EMF is almost sinusoidal, while the EMF for the extreme operating conditions presents insignificant signs of harmonic distortion, indicating the operation at the knee of the magnetizing curve.

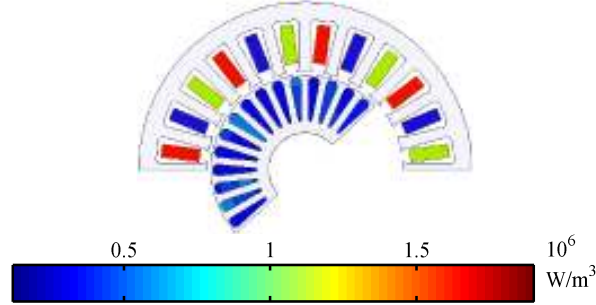


Figure 3. Power loss density distribution under normal operation at 20 ms 1.2Nm.

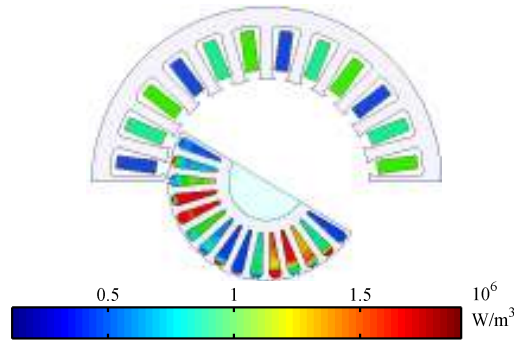


Figure 4. Power loss density distribution under extreme operating conditions at 100 ms.

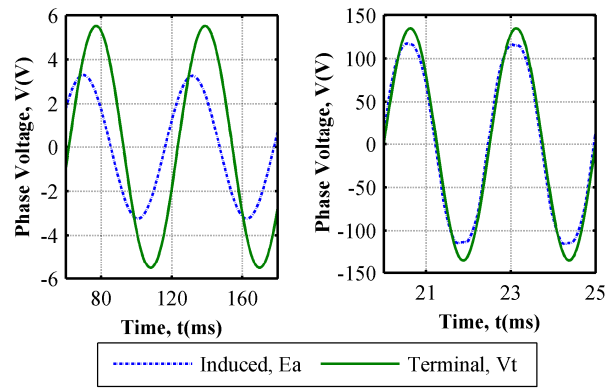
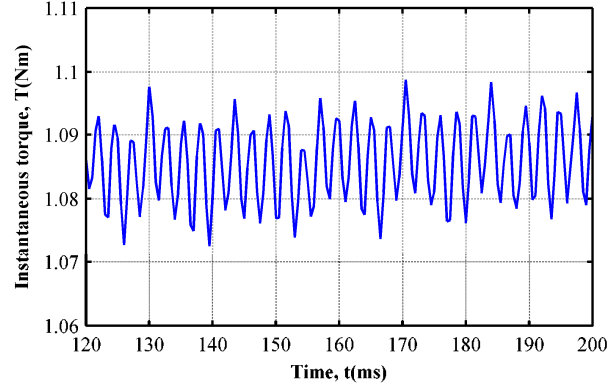


Figure 5. Induced and terminal phase voltage.

The torque ripple for the normal operation is below 2 %, as shown in Fig. 6, which is in a quite satisfying level. The selection of the stator and rotor numbers of slots is important reducing parasitic torque, additional losses, noise and vibration [15-18]. However, the construction of multi-pole and small in size machines delimits the available and feasible stator and rotor slots combinations [19-21]. Figure 7 depicts the instantaneous torque profile versus time for the normal operation.



**Figure 6. Instantaneous torque profile ( $T_{mean} = 1.085$  Nm).**

In order to identify the most appropriate correspondence between the stator and rotor numbers of slots possible combinations have been examined considering 24 stator slots mainly for construction limitations. The cross section of the copper bars and the rotor bore has been kept constant so as to deduce safe comparable results under the equal output torque.

After increasing significantly the rotor slots then the rotor teeth are heavily saturated affecting the torque ripple. Moreover, in such space-limited applications, a balance of the manufacturing feasibility and the most effective theoretical approach should be followed. It was evident that the 30 slots in rotor benefit from the increased slot number constituting also a satisfactory version.

Another important factor necessary to be taken into account is the rotor moment of inertia, which improves dynamic performance. The existence of the copper in the rotor slots deteriorates machine speed variations. Fig. 8 shows the instantaneous torque profile versus time considering a direct start for the extreme mode of operation counting also the mechanical vibrations. The total rotor moment of inertia is however below  $5e-4$  kg m<sup>2</sup>.

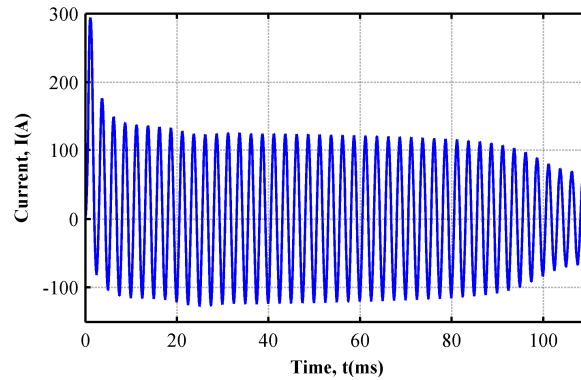


**Figure 7. Instantaneous current profile under direct start without loading.**

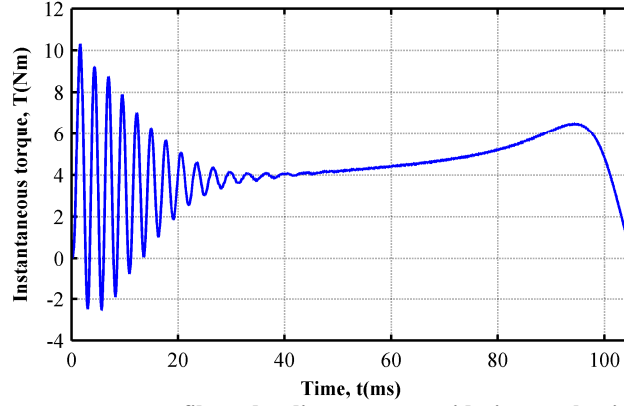


**Figure 8. Instantaneous torque profile under direct start considering mechanical part vibrations.**

- Permanent magnet actuator case

The winding configuration adopted for the PM actuator is the non overlapping single layer as concentrates the most benefits of the investigated winding topologies. The alternate teeth wound winding is considered a more favorable choice, however presents some drawbacks. The number of poles and slots has to be chosen carefully, otherwise the winding factor may be low, the torque ripple and the rotor losses high and the machine may be quite noisy. In order to indentify which winding layout, alternate teeth wound and all teeth wound, and the numbers of rotor poles and stator slots, different winding topologies have been examined by using the time-stepping FE analysis. Table 2 summarizes the main characteristics of some of the examined winding layouts considering identical embrace and thickness of the magnet configuration under the same voltage supply.

		Winding layout	Rotor poles	Torque ripple (%)	Winding factor
Single	a.	B A A' C' C B...	20	2.24	0.966
	g.	B A A' A A' C' C' C B...	22	1.55	0.958
	c.	B A A' A A' C' C' C B...	26	1.39	0.958
	e.	B A A' C' C B...	28	1.28	0.966
Double	b.	B'A A'A' AC' CC C'B...	20	1.72	0.933
	d.	B'A A'A' AA A'A' AC' CC...	26	1.06	0.950
	f.	B'A A'A' AC' CC C'B...	28	0.91	0.933
	h.	B'A A'C C'B...	32	4.16	0.866

**Table 2. Winding layout characteristics.**

In PM machines which have fewer stator slots than rotor poles, the MMF harmonic component that interacts in the mean torque production is not the fundamental but a higher harmonic component of the same order as the number of pole pairs. For this specific application and requirements, the 24 stator slots and 28 rotor poles single layer

fractional slot machine topology has been selected exhibiting low torque ripple with high winding factor, and subsequently, higher EMF capacity. Fig. 10 depicts the output torque profile for different winding layouts, single or double layer. The results are tabulated in Table 2.

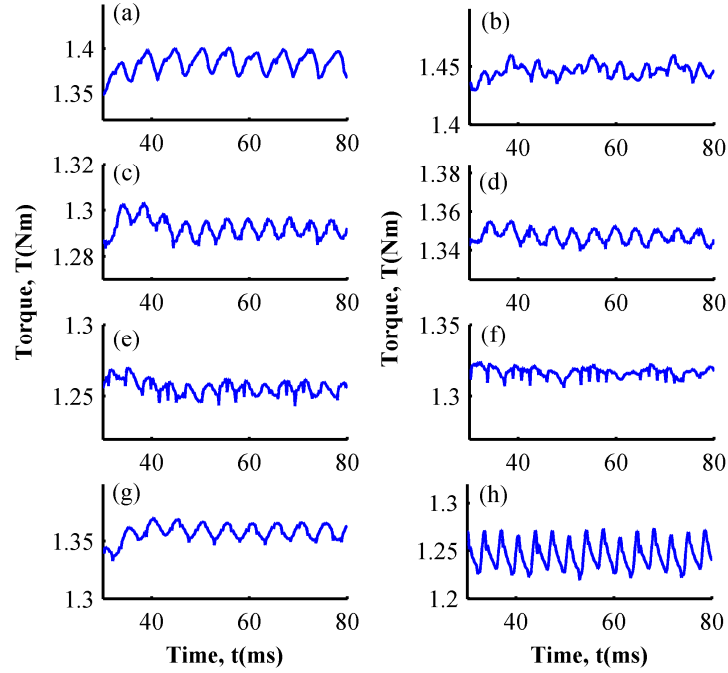
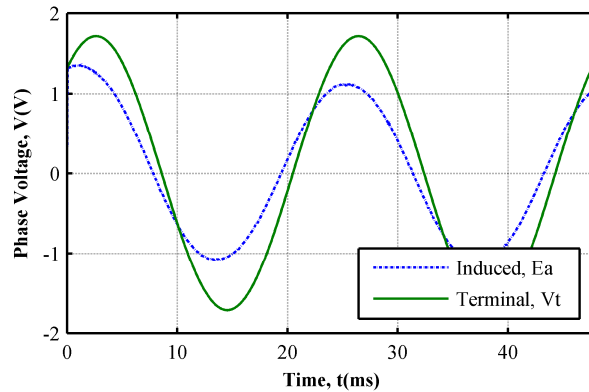


Figure 9. Output torque profile for different winding layouts, alternate teeth wound (left) and all teeth wound (right).

It is important for the machine operation to be capable of being further loaded in order to meet the requirements of the extreme loading condition. The torque angle, under normal operation, is approximately equal to 30 degrees and the EMF is absolutely sinusoidal, which is mainly due to the unsaturated stator and rotor core materials. Fig. 11 depicts the induced and terminal phase voltage considering a sinusoidal voltage supply at the machine terminals.

Under the extreme operating condition, the maximum torque at maximum speed is significantly higher than the specified torque for the normal operation.



**Figure 10. Induced and terminal phase voltage.**

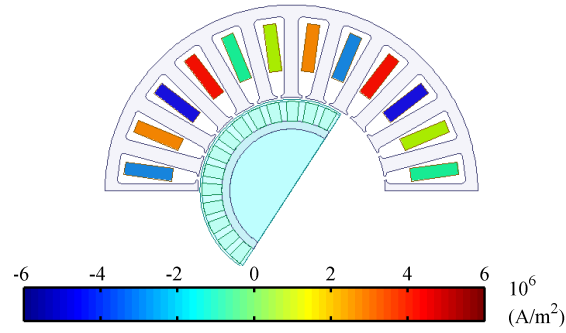


**Figure 11. Current density distribution under normal operation at 45 ms.**

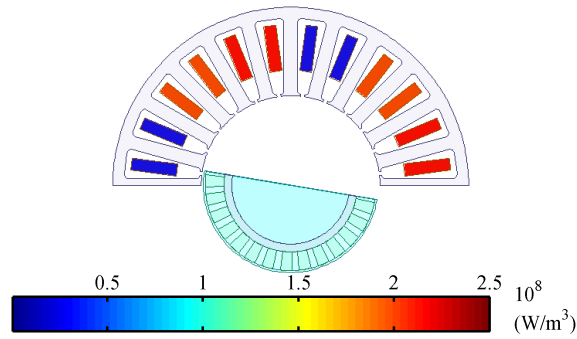


**Figure 12. Power loss density distribution under extreme operating conditions at 4.5 ms.**

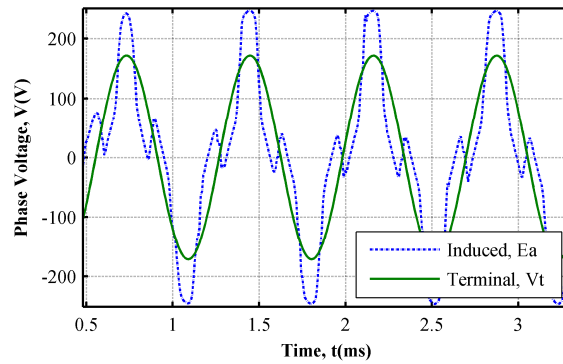


**Figure 13. Induced and terminal phase voltage.**

The mean flux density in the stator tooth is about 2 T leading the stator and rotor laminations to high saturation levels as shown in Fig. 12.

Subsequently, the highly saturated core affects the induced EMF presenting a 3rd harmonic component which equals to the 50.8% of the fundamental component. Fig. 13 shows the induced EMF for the extreme operating condition.

- Results and discussion

IM machines' disadvantages originate primarily from the absence of independent electromagnetic excitation in the rotor. From the preceded analysis it has been shown that the establishment of the rotor magnetic field demands higher current density to flow into the stator slots for the equal output torque levels thus deteriorating overall IM situation compared to the PM machine.

PM actuator demanded the one third of the total length, meeting the specifications, while the IM required the total available length. However, PM machine, under the extreme operating condition, necessitates stator and rotor core heavy saturation in order to achieve the desirable output torque, presenting distorted induced EMF and currents. Unlike the PM machine, the IM core saturation level is lower, due to the fact that the magnetic field in the rotor has already been established, thus having the capacity of being more loaded. It is worthwhile to be mentioned that topology optimization has been carried out for the normal operation for the two machine types. Table 3 summarizes the main PM and induction actuator characteristics for the normal operation.

Quantity	Value	
	PMM	IM
<i>Current density, <math>J</math> (A/mm<sup>2</sup>)</i>	4.14	4.05
<i>Depth, <math>l</math> (mm)</i>	40	120
<i>Number of conductors</i>	47	11
<i>Number of branches</i>	4	1
<i>Volume, <math>V</math> (m<sup>3</sup>)</i>	1.14e-4	4.55e-4
<i>Torque density, (kNm/m<sup>3</sup>)</i>	10.5	2.42
<i>Stator slots</i>	24	24
<i>Rotor slots</i>	-	30
<i>Poles</i>	20	8

**Table 3. PM and Induction actuator characteristics.**

Furthermore, in high performance applications, it is common to operate more than one machine in the same shaft for safety and reliability reasons contributing to a fault tolerant system. Therefore, under a machine fault, the remaining machines have to operate overloaded to substitute the fault machine operation and not to be hindered. The IMs benefit from the absence of rotor excitation exhibiting zero braking torque under short circuit fault. Fig. 15 illustrates this important disadvantage of the PM machines. Under a three phase short circuit at 20 ms, the IM presents almost zero braking torque after 40 ms. On the contrary, the PM machine continues to contribute with high braking torque of the value of 0.5 Nm.

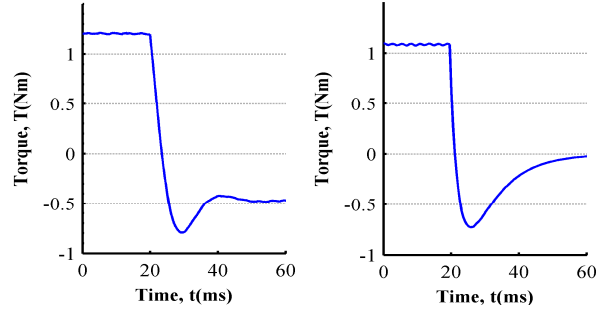
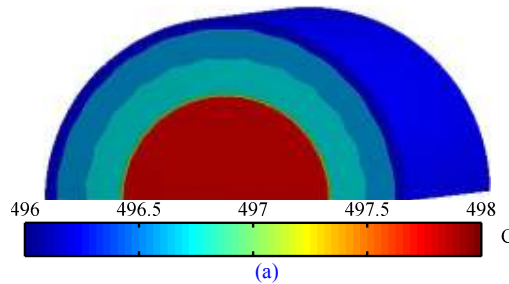


**Figure 14. Instantaneous torque under three phase short circuit fault considering constant speed load. (a) PM machine (b) IM**

These two actuator types exhibit intense differences and complementary advantages leading to a final choice depending on the type of the individual application. It may be noted that, for specific applications, the equal thermal evacuation criterion has to be taken into account. Due to the heavy environmental conditions, the contribution to the temperature rise is important. Thermal analysis results, shown in Fig. 16, demonstrate that each configuration presents almost equal heat flux levels. To that respect the PM configuration is favored as it involves important size and weight reduction through the same thermal constraints.

#### ▪ Conclusions

During EMAS project a comparative analysis between PMM and IM actuators for autonomous on board systems has been carried out. Different combinations of rotor-stator slots for the IM, and different winding layouts for the PMM have been modeled, and performances are compared. The optimum IM configuration, featured by the absence of rotor magnetic field, required larger dimensioning and weight than the respective PMM one, for the same thermal evacuation ratio. However, the IM case presented lower braking torque and short-circuit currents with respect to the PMM case, leading the final choice of the actuator technology to an overall system considerations dependent problem. In the present analysis by using the same thermal evacuation criterion the PM configuration was more favorable.





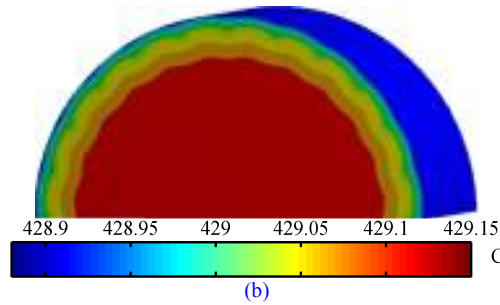


Figure 15. Steady state temperature distribution. (a) Induction actuator. (b) PM actuator.

- Potential impact and the main dissemination activities and exploitation of results.

The use of electrically powered actuators integrating speed and position sensors is expected to enable to save weight, and to increase engine monitoring and diagnostics. Moreover, EMAS project findings will allow to reduce the size of components of generation equipment as well as to achieve significant reduction in maintenance. Another aspect of EMAS developments is increased reliability because safety has a great impact in aeronautic transports.

The main objective of the dissemination plan was to guarantee proper diffusion of knowledge and project results. The dissemination process was handled so as to spread information among all potentially concerned stakeholders and all levels of policy-makers: such as aeronautics supply industry, Safety and certification bodies, Standardization bodies, Engineering Organizations, European and national policy makers, Universities, Schools and European citizens. The activities that disseminated EMAS results are as follows:

- Presentations in International Conferences and Workshops.
  - P. Kakosimos, E. Tsampouris and A. Kladas, “*Design considerations in actuators for aerospace applications*,” IEEE Biennial Conference on Electromagnetic Field Computation CEFC 2012, Oita, Japan, November 2012.
  - P. Kakosimos, E. Tsampouris, A. Kladas and C. Gerada, “*Aerospace actuator design: a comparative analysis of permanent magnet and induction motor configurations*,” International Conference on Electrical Machines ICEM 2012, Marseille, France, September 2012.
  - P. Kakosimos, E. Tsampouris, C. Patsios and A. Kladas, “*A comparative study of PM and induction motor actuators for on board applications*,” 1<sup>st</sup> International MarineLive Conference on “All Electric Ship”, Athens, Greece, June 2012.